Kinetics of FO_2 with NO, NO_2, O_3, CH_4, and C_2H_6

Zhuangjie Li, Randall R. Friedl, and Stanley P. Sander*

Jet Propulsion Laboratory, California Institute of Technology
Pasadena, California 91109

Submitted to the Journal of Physical Chemistry

01/27/95

*Author to whom correspondence should be addressed

Abstract

The kinetics of the reactions $FO_2 + NO \rightarrow$ Products (11) and $FO_2 + NO_2 \rightarrow$ Products (12) have been studied as functions of temperature at 1 Torr total pressure using a discharge-flow mass spectrometric technique. The measured rate coefficients, expressed in Arrhenius form, are k_{11} = (7.5 ± 0.5) x 10^{-12} exp[(-688 ± 145)/T] cm^3 $molecule^{-1}$ s^{-1} for 190 K <1<298 K and k_{12} = (3.8 ± 0,8) x 10-] ^{1}exp[(-2042 ± 56)/'1] cm^3 $molecule^{-1}$ s^{-1} for 260 K < T < 31 5 K, The observed temperature dependencies of the rate coefficients indicate that the reactions occur primarily by simple bimolecular, rather than termolecular, mechanisms. Mass spectral product studies arc consistent with bimolecular processes involving F atom extraction from FO_2. Upper limits for the rate coefficients of $FO_2 + O_3 \rightarrow$ Products (13), $FO_2 + CH_4 \rightarrow$ Products (14), and $FO_2 + C_2H_6 \rightarrow$ Products (15) have also been determined with the same experimental system at room temperature: $k_{13} < 3$ x 10^{-15} cm^3 molecule-l s^{-1}, $k_{14} < 2$ x 10^{-16} cm^3 molecule-] s^{-1}, and $k_{15} < 4$ x 10-] ^{6} cm^3 $molecule^{-1}$ S-l. As part of the $FO_2 + O_3$ study, an investigation of the reaction $FO + O_3 \rightarrow FO_2 + O2$ (6) was conducted. An upper limit of $k_6 < 1$ x 10^{-14} cm3 $molecule^{-1}$ s] has been obtained for the FO reaction, The implications of these results for fluorine oxide chemistry in the atmosphere are discussed.

introduction

The **presence** of fluorine containing compounds (e.g. 1 lF and COF_2) in the Earth's atmosphere is thought to be due solely to the decomposition of man-made chemicals such as chlorofluorocarbons (CFCs) and hydrofluorocarbons (HFCs).[1] The effect on atmospheric ozone of reactive fluorine-containing intermediates produced during CFC and HFC decomposition has attracted significant interest recently, although far less than the analogous chlorine intermediates.[2,3] Recently, the possibility of a catalytic cycle involving CF_3O_x has been proposed.[4] Based on kinetics studies of the relevant chain propagating and terminating reactions, model calculations conclude that the impact of this cycle on ozone is insignificant.[5-8] Earlier, Stolarski and Rundel[9] considered the effect of F atoms on ozone and concluded that the catalytic efficiency of a cycle involving F and FO,

$$F + O_3 \rightarrow FO + O_2 \quad (1)$$

$$FO + O \rightarrow F + O_2 \quad (2)$$

---

net $$O + O_3 \rightarrow 2\,O_2 \quad (3)$$

was less than 10-4 that of the corresponding chlorine cycle, due primarily to the rapid F atom termination by RH1 species,[9]

$$F + RH1 \rightarrow HF + R \quad (4)$$

where R = 011, CH_3, H etc., and the HF product is a stable fluorine reservoir.

Subsequent to the Stolarski and Rundel calculation, several laboratory investigations have shown that F atoms react at an appreciable rate with molecular oxygen to form FO_2.[10-12]

$$F + 1\,02 + M \leftrightarrow FO_2 + M \quad (5,-5)$$

In addition, the FO_2 product has been found to be relatively stable thermally, Based on the experimental kinetics anti thermochemical parameters for reactions 5 and -S, one estimates that the reaction of atomic fluorine with molecular oxygen is over two orders of magnitude faster than any other atmospheric fluorine atom removal process and that the equilibrium ratio of $[FO_2]$ to [F] in the stratosphere is greater than 10^4.

Recognition of the potential atmospheric presence of FO_2 has led to suggestions of atmospheric ozone depletion cycles involving FO_2.[13,14] One such cycle involves the reactions of FO and FO_2 with 03.

$$FO + O_3 \rightarrow FO_2 + O_2 \quad (6)$$

$$FO_2 + O_3 \rightarrow FO + 20'2 \quad (7)$$

$$\text{net} \quad O_3 + O_3 \rightarrow 3O_2 \quad (s)$$

The impact of this cycle on ozone will depend upon the kinetics of reactions 6 and 7 relative to the removal rates of FO and FO_2 radicals by other atmospheric species such as NO, NO_2, and hydrocarbons, In the current study we have investigated the kinetics and product yields of FO_2 reactions with 03, NO, NO_2, CH_4, and C_2H_6 using the discharge-flow mass spectrometric technique. We have also examined the kinetics of the reaction of FO with O_3. In this report wc present the results of these studies and discuss the implications of these results for stratospheric ozone. We also compare our results with those of Sehc.steel et al.[15] that were obtained using pulse radiolysis/UV absorption spectroscopy and that were reported during the course of our investigation .

Experimental

The experimental apparatus used for kinetics studies of reactions involving FO_2 is shown in Figure 1. The reactor consisted of a 60-cm-long, 2.54 -cm-o. d Pyrex tube coated with halocarbon wax to reduce F02 wall loss. The reactor temperature was varied between 190 and 3is K by circulation of cooled methanol or heated ethylene glycol through an outer Pyrex jacket, The temperatures of the circulating fluids were measured by a thermocouple located in the liquid reservoir and controlled to a precision of ±2 K by use of a thermostat ted heat exchanger. A steady state gas flow (total pressure, of 1 torr) was established in the reactor by connection to a 50 cfin mechanical pump (Welch 1398). Helium was used as the main buffer gas and was admitted through sidearm located upstream of the reactor. The resulting reactor flow velocities ranged between 900 and 4000 cm s-1; the corresponding gaseous residence t imes within the reactor were

between 65 and 15 ms. A liquid nitrogen trap was placed downstream of the reactor in order to protect the vacuum pump from corrosive reactants ancl reaction products.

Mass spectrometric detection of reactants and products was carried out by continuous sampling at the downstream end of the flow tube through a thi ec-stage beam inlet system. The mass spectrometer (Extrel Model C50) consisted of an electron-impact ionizer, a quadruple mass filter, and a channeltron. Beam modulation was accomplished with a 200 Hz tuning fork type chopper placed inside the second stage of the mass spectrometer. Ion signals from the channeltron were sent to a lock-in amplifier that was referenced to the chopper frequency. The amplified analog signals were converted to digital form (Analog Devices RTI/8 15) and recorded on a microcomputer.

Excess reagents were added into the reactor through a 120 cm-long, 0.63 cm-o.d. sliding Pyrex injector tube that was concentric with the reactor tube. The sliding injector was also coated with halocarbon wax on the outside, Contact times between the excess reagents and the limiting reagent (typically FO_2) were varied by movement of the injector,

FO_2 was generated by reaction of atomic fluorine ($[F] \leq 10^{12}$ molecule cm^{-3}) with molecular oxygen ($5 \times 10]^{5}$ molecule $cm^{-3} \leq [O_2]$)

$$F + O_2 + M \rightarrow FO_2 + M \qquad (5)$$

inside a 40-cm-long, 2-cm-o. d Pyrex tube located upstream of the main reactor. Since the formation of FO_2 involves a three body process, the FO_2 "pre-reactor" was separated from the main reactor by a pinhole in order to establish a He pressure difference between the two sections of approximately 100 torr. Conversion of F to FO_2 was also enhanced by cooling the pre-reactor to 260 K at which temperature the equilibrium $[FO_2]/[F]$ ratio was estimated to be greater than 20. Temperature control of the pre-reactor was accomplished in the same fashion as for the main reactor, however, the two temperature control systems were independent of one another,

The mass spectral signal from F02 was observed at both m/e = 51 (FO_2^+) and m/e = 35 (FO^+). The relative intensities of the fragments were largely independent of electron impact energy except at the lowest energies ($\leq$ 30 eV) where the FO_2^+ fragment was substantially more

intense than the FO^+ fragment (see Table I). Consequently, operation at the lowest possible impact energies provided a suitable means to detect FO_2 and FO radicals simultaneously.

The assignment of the ion mass peaks to FO_2 was checked by reacting isotonically labelled molecular oxygen, i.e. 3602 instead of $^{32}O_2$, with atomic fluorine. The resulting mass spectral signals were observed at m/e=55 and 37 with approximately the same intensities, for a given F atom concentration, as those obtained from the normal isotope Formation of fluorine peroxide, F_2O_2, in the pre-reactor by reaction of]; atoms with FO_2

$$F + FO_2 + M \rightarrow F_2O_2 + M \qquad (9)$$

k_9=1. lx] 0^{-13} c m^3 molecule^{-1} s^{-1} ^{10}

is one possible source of mass spectral interference that was not addressed by the isotopic substitution experiment. However, the use of large [02] to [F] ratios in the pre-reactor was expected to minimize this interference. In support of this prediction we found that ten-fold variations in the 02 concentration had little effect on the observed fragment ion intensity ratios.

Absolute concentration calibrations of mass spectral signals were required for control of the experimental conditions and for extraction of reliable kinetic parameters from temporal profiles of reactants and/or products. In this study, N02 (m/e= 46), NO (m/e= 30), and CH_4 (m/e= 16) signals were calibrated by comparison with measured flows of these species. FO_2 was calibrated by chemical titration of known amounts of atomic fluorine by molecular oxygen. F atom concentrations were determined by reaction with excess CH_4 and subsequent monitoring of the change in the CH_4 signal. Calibration of O_3 was also achieved by a chemical conversion method; in this case the O_3 was stoichiometrically converted to N02 by reaction with excess NO. Detection limit for the molecules and radicals of interest were found to range between 1 xl 0^9 and **3x109** molecule cm^{-3}. For some of the slow reactions studied in this work, excess reactant concentrations were obtained by measuring pressure increases inside the reactor upon addition of the reactants.

The gases used in this work were obtained mainly from Matheson: He, 99.99%; 0_2, 99.98%; NO, 99%; N02, 99.5%; CH_4, 99.97%; and C_2H_6, 99.96%. I sotopically labeled oxygen $^{36}02$ was obtained with 98% purity from Cambrige Isotope 1 laboratories. F2 (5% in He) was

obtained from Spectra Gases Inc. NO was further purified by passage through an Ascarite trap. The presence of trace NO impurities in the N02 samples was recognized as a significant complication to the kinetics studies of FO_2 with N02. We employed two schemes to purify the N02 samples: 1) multiple low temperature(195 K) distillations to remove the volatile NO, and 2) addition of 02 to the sample in order to convert the NO impurity into N02. Consistent results were obtained using samples derived from either purification method. Ozone was produced in an ac discharge (Welsbach Model T-408) of 02 and stored on silica gel at 195 K. During the experiments, O_3 was maintained at 195 K and bubbled into the reactor with a measured flow of He, After passage through the reactor ozone was heated to approximately 900 K in a 50-cm-long quartz tube which was wrapped with nichrome wire and located upstream of the liquid nitrogen trap. Only small amounts of undecomposed O_3 survived the heated region and were collected in the liquid nitrogen trap; the collected samples were removed to a ventilation hood along with the liquid nitrogen dewar at the end ofexperirnents.

Results

Kinetics measurements were accomplished by monitoring the decay of F02 in the presence of excess reactants as a function of contact time. For most of the reactions F02 was introduced into the reactor through a fixed side arm and the excess reagents were added through the sliding injector. In the NO and N02 cases, several measurements were performed by adding FO_2 through the sliding injector. Using the low-pressure limiting rate constant for reaction S and the equilibrium constant at room temperature, [10] the lifetime of F02 in our flow tube was estimated to be greater than 1 second, which is substantially longer than the FO_2 residence time in the flow tube. This was consistent with the fact that FO_2 signal levels were largely unaffected by the change in flow path, indicating that FO_2 disproportionation and wall loss were essentially negligible on the time scales of the steady state flow apparatus.

The method required to obtain kinetics rate parameters from measured concentration decays in a steady state flow tube apparatus is well known.[6-18] Following this method, first-order decay rates, k', were determined from slopes of plots of the logarithm of FO_2 signal vs.

injector distance and the measured flow velocities. The observed decays were corrected for axial diffusion and for loss of F02 on the injector according to eq (I),

$$k^{1}=k'(\ ]\ -t\ k'D/v2)+k_p \qquad (I)$$

where D is the diffusion coefficient, V^2 is the mean bulk flow velocity, and k_p is the first order loss of F02 on the outside surface of the sliding injector. I 'or experiments where F02 was added through the sliding injector, the observed decay were corrected for both axial and radial diffusion effects according to eq (l I),

$$k^{1} = -(\frac{2D}{r^2})(\sum_{n=0}^{\infty} 2n\,B_n / \sum_{n=0}^{\infty} B_n) \qquad (11)$$

where r is the reactor radius, and B_n are k'-dependent diffusion coefficients.[17] The diffusion coefficient for FO_2 was estimated using the empirical equation developed by Fuller et al. [19] The estimated D value varied from 0.24 atm cm^2 s^{-1} at 190K to 0.60 atm cm^2 s^{-1} at 31 SK, Corrections for axial diffusion were always less than 1%, and losses of F02 on the injector and reactor surface were always measured to be less than 1 s^{-1}.

'l'he bimolecular rate constants, k, were obtained from slopes of linear least-square fits to the plots of k^1 vs. reactant concentration. Reaction activation energies and A-factors for reactions of FO_2 with NO and N02 were determined from slopes and intercepts of plots of the natural logarithm of k *vs.* reciprocal temperature.

Reaction of FO_2 with NO.

Typical room temperature decays of FO_2 in the presence of NO are shown in Figure 2. Initial FO_2 concentrations ranged between 5x1011 and $3x10^{12}$ Cm-3; NO concentrations were varied bet ween **2x10] 2** and $1.6x10^{14}$ cm^{-3}. Observed first order decay rates of FO_2, plotted against NO concentration in Figure 3, varied fi om appi oximat ely 1 to 130 s^{-1}. At slow flow velocities ($\leq$ 1000 cm s^{-1}) and for NO concentrations greater than approximately 1 x 1014 molecule cm^{-3}, it was necessary to correct the observed FO_2 decays foi the effects of the reaction between NO and F_2[20-22]

$$F2 + NO \rightarrow F + FNO \qquad (1o)$$

k_{10}=1.2x1 0-14 cm^3 molecule-l s^{-1} 22

Under the latter conditions, reaction (1 O) served as a small, yet significant, source of FO_2 (due to F+- *02).* The corrections for this effect, as determined from computer simulations, were less than 10%. After correction of these data, the resulting room temperature rate coefficient was determined to be (8.5±1.3) x 10-13 cm^3 $molecule^{-1}$ s^{-1}, where the quoted uncertainty is at the 95% confidence limit.

The temperature dependence of the rate coefficient was determined over the temperature range 190 to 298 K. FO_2 decay rates at various temperatures are shown in Figure 3. The set of experimentally determined rate coefficients is shown in Table 1 and Figure 4. The direct or "positive" dependence of the rate constant on temperature suggests that the reaction proceeds by a bimolecular rather than termolecular mechanism.[23,24] Fitting the data to a simple Arrhenius expression yields,

$$k_{11}=(\text{'7,5*5})\text{x}10\text{-}1^{2}\exp(-688\pm145/T)\ cm^3 molecule^{-}\ s^{-1}.$$

The apparent lack of a termolecular reaction channel, i.e.

$$F02 + NO + M \rightarrow FO_2NO + M \cdot \qquad (ha),$$

as suggested by the positive dependence of the reaction rate coefficient on temperature, was further supported by our failure to detect FO_2NO^+ (m/e = 81) or NO_3^+ (m/e = 62). Assuming that the detection threshold for FO_2NO at either of the ion peaks is comparable to that of $HONO_2$, we place an upper limit of 0.10 on the branching ratio k_{11a}/k_{11}.

Among possible bimolecular reaction channels only the pathway involving F atom abstraction from F02,

$$F02 + NO \rightarrow FNO + 02 \qquad (1\,lb),$$

is exothermic, and therefore likely to occur. The O atom abstraction pathway,

$$FO_2 + NO \rightarrow FO + NO_2 \qquad (11c)$$

is endothermic by approximately 6 kcal $mole^{-1}$. We confirmed the minor role of reaction channel 11 c through observations of the N02 product. For these experiments we employed isotonically labeled $F^{36}O_2$ and detected the resulting $N^{16}O^{18}O^+$ (m/e=48) following titration of the $F^{36}O_2$

with NO. The use of labeled reactant was designed to allow differentiation of NO_2 produced from the reaction from that contained as an impurity in the NO sample. In all trials the amount of labeled NO_2 observed was less than 3°A of the initial FO_2 concentration. Accordingly, the branching ratio for reaction 11 c, k_{11c}/k_{11}, is <0.03. Based on the branching ratio results for channels 11a and 11 c we conclude that the branching ratio for 11 b is nearly unity. However, wc were unable to confirm this conclusion experimentally since the FNO^+ (m/e= 49) product was strongly fragmented in the ionizing region and its fragments, F^+ and NO^+, were masked by the mass spectral features of the reactants.

Reaction of FO_2 with NO_2

Decays of FO_2 in the presence of N02 were readily observable, although much smaller than in the NO case (see Figure 5). First-order decay rates of F02 were obtained as a function of N02 concentration at several temperatures. (see Figure 6) The N02 concentrations, as measured either by a calibrated flow meter or by monitoring the pressure increase upon addition of N02, were corrected for dimerization using,

$$[NO_2]_{cor} = \frac{-0.5 + \sqrt{0.25 + [NO_2]_m \, 2K_{eq}}}{2K_{eq}} \qquad \text{(III)}$$

where $[NO_2]_{cor}$ is the corrected N02 concentration, $[NO_2]_m$ is the measured $N0_2$ concentration, and K_{eq} is the equilibrium constant for dimerization. The expressions for K_{eq} was obtained from the evaluation of DeMore et al.[25] In the temperature range of 260-315 K the N02 concentration correction was less than 3%. The relatively large amounts of N02 gas required for these experiments were obtained directly from a liquid N02 sample, Onc difficulty with this method was the maintenance of a steady gaseous N02 flow rate due to variations in the gas/liquid steady state. 'l'his difficulty manifested itself as a somewhat larger uncertaint y in the determination of the N02 gas phase concentration.

The experimentally derived bimolecular rate constants for reaction 12 are listed in Table 2 and displayed as a function of temperature in Figure 7. A fit of the rate coefficient data to an Arrhenius expression yields

$$k_{12} = (3.8 \pm .8) \times 10^{-11} \exp(-2042 \pm 56/T) \text{ cm}^3 \text{ molecule}^{-1} \text{ s}^{-1}$$

Analogous to the NO reaction (reaction 11), the observed positive temperature dependence of the N02 reaction suggests the occurrence of a bimolecular (reaction 12a), rather than a termolecular mechanism (reaction 12b).

$$FO_2 + NO2 \rightarrow FNO_2 + O2 \qquad (12a)$$

$$FO2 + NO2 + M \leftrightarrow FO_2NO_2 + M \qquad (12b,-12b)$$

No experimental verification of the bimolecular reaction mechanism could be obtained, however, since the FNO_2^+ (m/e = 65) ion is highly fragmented in our apparatus and the resulting fragment ions are masked by reactant-related ions. The observed absence of $FO_2NO_2^+$ (m/e = 97) is consistent with the lack of a termolecular channel, but one can not rule out the possibility that F02N02 adduct is either weakly bound or strongly fragmented upon electron impact at 30 eV.

Reaction of FO_2 with 03, CW4, *and* C_2H_6.

The reactions

$$FO2 + O_3 \rightarrow \text{products} \qquad (13)$$

$$FO_2 + CH_4 \rightarrow \text{products} \qquad (14)$$

and

$$FO_2 + C_2H_6 \rightarrow \text{products} \qquad (15)$$

were also studied in this work. No significant F02 decay ($k' \leq 1\ s^{-1}$) was observed for 03, CH_4, and C_2H_6 concentrations of $\leq 5 \times 10^{14}$ molecule cm^{-3}, $\leq 5 \times 10^{15}$ molecule cm^{-3}, and $\leq 3 \times 10^{15}$ molecule cm^{-3}, respectively, and for reaction times up to 70 ms. In addition, we did not observe any of the expected products such as FO(m/e=35), OH(m/e= 16), and HF(m/e=20). Based on these observations the derived upper limits for the bimolecular rate constants are $k_{13} < 3 \times 10^{-15}$ cm^3 molecule-1 S-1, $k_{14} < 2 \times 10^{-16}$ cm^3 $molecule^{-1} s^{-1}$, and $k_{15} < 4 \times 10^{-16}$ cm3 $molecule^{-1} s^{-1}$.

For the ozone reaction we considered the possibility of FO_2 regeneration by the secondary reaction of FO with *03,* i.e.

$$FO_2 + 03 \rightarrow FO + 2O_2 \quad (7)$$

$$FO + 03 \rightarrow FO_2 + O_2 \quad (6)$$

$$\text{net} \quad 03 + 03 \rightarrow 3O_2 \quad (8)$$

The occurrence of the FO reaction could lead to FO_2 steady state formation and catalytic ozone destruction. If a steady state were established the condition would be described by

$$[FO_2]_{ss}/[FO]_{ss} = k_6[O_3]/k_7[O_3] = k_6/k_7 \quad (Iv)$$

or

$$[FO_2]_{ss}/[FO_2]_o = k_6/(k_6+k_7) \quad (v)$$

where $FO_2]_{ss}$ and $[FO]_{ss}$ are the steady state concentrations and $[FO_2]_o$ is the concentration prior to reaction. As demonstrated by the above expressions, the steady state concentrations will not depend on the 03 concentration. The absence of both an observable FO_2 decay and an appreciable FO production in the presence of 03 can be rationalized in terms of the above mechanism only if $k_6 >> k_7$. In order to check for this possibility we inverted the initial condition of the reaction system by producing FO, rather than F02, using the reaction of atomic fluorine with excess 03. A rapid reaction between F() and 03 would result in depletion of the FO and production of FO_2. However, no appreciable decay of FO was observed and only a small increase in F02 was detected. In addition, the concentration of 03 was found unchanged. These observations confirm that the reaction of F02 with 03 does not occur to any significant extent in our system. Based on our data we derive an upper limit of $k_6 < 1 \times 10^{-15}$ cm^3 molecule^{-1} s^{-1} for the reaction of FO with O_3.

Discussion

Reaction rate constants obtained in this study are listed in Table 2 along with room temperature values of several FO_2 and FO reactions reported recently by Sehested et al.[15] The upper limits obtained in this study for the reactions of FO and FO_2 with 03 and FO_2 with CH_4

are entirely consistent with those obtained by Sehested et al. In the case of the $F02 + CH_4$ reaction the upper limit value obtained in the present work represents a factor of five lowering of the previous limit obtained by Sehested et al.

The room temperature values of k_{11} and k_{12} obtained by Sehested et al. are approximately 75% and 150% higher, respectively, than those obtained in the present work. The discrepancy between the values of k_{12} may be attributable to the presence of NO impurity in the N02 sample employed by Sehested et al. As mentioned above we discovered substantial contamination of our N02 samples by NO. The purity of the NO_2 sample used by Sehested et al. is reported by the vendor to be >98%, however, thermal and or heterogeneous decomposition of the N02 during storage may result in increased amounts of NO. Based on our measured ratio of k_{11} to k_{12}, an NO impurity level of 3'% is sufficient to increase the apparent rate constant of reaction 12 by a factor of 2.5. We have found in our investigation that the level of NO impurity in a relatively old sample of N02 can approach 3%.

The measurements of Sehested et al. were carried out at substantially higher pressures (1 18 bar) than those used in the present work (0.001 bar). Accordingly, the rate constants measured by Sehested et al. might be compatible with our lower values if they include increased contributions from termolecular reaction channels. In the case of the N02 reaction, Sehested et al. found k_{12} to be invariant over the experiment al pressure range, This implies that reaction 12 either follows a purely bimolecular reaction path at all pressures or that the termolecular component is at its high pressure limit for pressures above 1 bar. The kinetics parameters associated with a potential termolecular channel are, as constrained by the low and high pressure observations, $k_0 \leq 3 \times 10\text{-}31$ cm^6 molecule^{-2} S^{-2} and $k_\infty \leq 1.05 \times 10\text{-}13$ cm^3 molecule^{-1} s^{-1}, In order to assess the plausibility of the low pressure limit we estimated the third-order rate constant for reaction 12b using Tree's approximate method,[26-28]

$$k_{rec}^{sc} = k_{diss}^{sc} K_{eq} \qquad (w)$$

and

$$k_{diss}^{sc} = Z_{LJ} \frac{\rho(E_0)RT}{Q_{vib}} \exp(-E_0/RT) F_E F_{anh} F_{ret} F_{corr} \qquad (w)$$

where k_{diss}^{sc} is the strong collision dissociation rate constant in the low-pressure second-order region, Z_{LJ} the Lennard-Jones collision frequency, $\rho(E_0)$ the density of states at the critical energy E_0, F_E, F_{anh}, Fret are the correction terms for the energy dependence of the density of states, anharmonicit y, and rotation, F_{corr} is the correction term (usu ally set to be 1) to account for coupling between the different types of degrees of freedom, Q_{vib} is the vibrational partition function, k_{rec}^{sc} is the association rate constant, and K_{eq} is the equilibr ium constant. Many of the required parameters for HO_2NO_2 were estimated from HO_2NO_2[27]

$$H02 + N02, \leftrightarrow \quad HO_2NO_2 \qquad (16, -16)$$

For instance, Q_{vib} was computed using all of the known HO_2NO_2 vibrational frequencies except for those corresponding to H-O stretching motions. The latter vibrational frequencies were replaced by estimates of the analogous F-O stretches. Z_{LJ} was evaluated using the same Lennard-Jones well depth and collision diameter as that of HO_2NO_2; and K_{eq} was estimated using the HO_2NO_2 entropy calculated by assuming a similar structure to that of H02N02. Using the H02N02 binding energy of 22 kcal mol^{-1}, the calculated value of k_{rec}^{sc} at 300 K for reaction 12b is 4.7x10-32 cm6 molecule-2 s^{-1}; a value that is consistent with the experimental constraint discussed above. The implied high pressure limit, however, is substantially lower than other analogous termolecular reactions of small radicals. I or example, the high pressure limit for HO_2NO_2 formation (reaction 16) is 4.7x10-12 cm^3 $molecule^{-1}$ S-l, Accordingly, we believe that the discrepancy between k_{12} values measured by us and by Sehested et al. cannot be rationalized in terms of the combined effects of a bimolecular and ter molecular channel. Further exploration of the possibility of a termolecular channel requires data at pressure ranges between 1 and 760 torr.

The present results allow us to compare the reactivity of HO_2 with other peroxy and peroxy-like species such as H02 and 03. As shown in Table 3, t he reactivity of HO_2 lies between those of HO_2 and 03 in the case of NO, but is significantly greater than both H02 and O_3 with respect to N02. Furthermore, when reacting with NO or O_3, HO_2 acts like an oxygen donor

while FO_2 appears to act as a fluorine donor. This latter behavior may arise from the bonding characters of these radicals. Figure 8 shows the highest occupied molecular orbital (HOMO) of both HO_2 and F02 radicals in 2A" ground state, as computed using GAUSSIAN 92 with H02 and FO_2 geometries optimized at QCISD(T)/6-311 G(d,p) and QCISI)(T)/6-31 G* levels of theory .3] For HO_2, the *ab initio* calculations predict that the interaction between the $3P_x$ orbitals on the oxygen atoms is antibonding while the interaction between the 2S orbital of hydrogen and the $3P_x$ orbital of oxygen is bonding. Foi F02, the interactions between the $3P_z$ orbitals on the oxygen atoms and the $3P_z$ orbitals on the fluorine and oxygen atoms are both antibonding. The antibonding character of the F and O atom interaction significantly weakens the F-O bond in F02 relative to the H-O bond in HO_2, and provides a rationale for the propensity of reactions involving FO_2 to occur by F atom abstraction.

A tmospheric Implications.

The earlier calculation of Stolarski and Rundel snowed that because the $[F]/[F_X]$ ($[F_X] = [F] + [FO] + [HF]$) ratio in the atmosphere is small the rate of ozone destruction per molecule of fluorine is insignificant even when the rate limiting step in a F-catalyzed removal cycle is fast (i.e. $k_{r.l.} = 5 \times 10\text{-}11$ cm^3 $molecule^{-1}$ s^{-1}). The potential significance of a catalytic cycle involving F02 derives from the fact that the atmospheric $[FO_2]/[F_X]$ ratio is nearly four orders of magnitude larger than the $[F]/[F_X]$ ratio. The kinetics results obtained in previous work [15] and confirmed here reveal slow processes for destruction of ozone by both FO_2 and FO. Sehested et al. [15] have derived analytical expressions for the chain lengths for ozone destruction from FO_2 and FO catalytic cycles. These calculations indicated that, on a per atom basis, fluorine is 10^3- 104 times less efficient at ozone destruction than the chlorinate. The smaller rate constant values for FO_2 + NO and N02 obtained here compared with the Schested et al. study do not significantly alter this conclusion but will change the partitioning of active fluorine radicals in favor of FO_2 to a small extent. Furthermore, if the reactions

$$FO_2 + XO \rightarrow FO + X + O_2 \quad (17)$$

$$FO + Xo \rightarrow FO_2 + x \quad (18)$$

net $2XO \rightarrow 2X + O_2$ (19)

(where X=H, Cl, Br) are fast, fluorine species may serve to accelerate ozone removal cycles involving HO_x, ClO_x, and BrO_x. Kinetics studies are needed on reactions 17 and 18 to assess this latter possibility

Acknowledgement

We thank Ole John Nielsen and his colleagues for a preprint of their work on F02 kinetics. This research was performed by the Jet Propulsion Laboratory, California Institute of Technology under contract with NASA, and was supported in part by the Alternative Fluorocarbon Environmental Acceptability Study,

References:

1. Atmospheric Ozone 1985, W. MO. Global Ozone Research and Monitoring Project, Report No. 16; 1985.

2. Alternative Fluorocarbon Environmental Acceptability Study, W.M. O. Global Ozone Research and Monitoring Project, Report No. 20; Scientific Assessment of Stratospheric Ozone, Vol 2, 1989.

3. Scientific Assessment of Stratospheric Ozone Depletion: 1991, World Meteorological Organization Global Ozone Research and Monitoring Project. Report No, 25.

4. Ko, M, K. W.; Sze, N. D.; Rodriguez, J.M; Weistenstein, D. K.; Heisey, C. W.; Wayne, R. P.; Biggs, P; Canosa-Mas, C. E.; Sidebottom, H, W.; and Treaty, J. *Geophys. Res. Lett.* 1994, 21, 101.

5. Ravishankara, A. R,; Turnipseed, A.A.; Jensen, N. R.; Barone, S.; Mills, M.; Howard, C. J.; and Solomon, S.; *Science*, **1994,** 263, 71.

6. Nielsen, O. J.; Sehested, J. *Chem. Phys. Lett.* **1993**, 213, 433.

7. Wellington, T. J.; Hurley, M. D.; Schneider, W.F. *Chem. Phys. Lett. 1993,* 213, 442.

8. Maricq, M. M,; Szente, J. *Chem. Phys. Lett.* **1993,** 213, 449.

9. Stolarski, R. S. and Rundel, R. D. *Geophys. Res. Lett. 1975,* 2, 443.

10. Pagsberg, P.; Ratajczak, E.; Sillesen, A. *Chem. Phys. Lett. 1987,* 141, 88.

11. Lyman, J. L,; Holland, R. *J. Phys. Chem. 1988,* 92, 7232.

12. Ellermann, T.; Sehested, J.; Nielsen, O. J.; Pagsberg, P.; Wellington, "1'.1'. *Chem. Phys. Lett.* 1994,218,287.

13. Francisco, J, S. *J. Chem. Phys. 1993,* 98,2198.

14. Francisco, J. S.; Su, Y. *Chem. Phys. Lett.* **1993,** 215, 5S.

1 S. Sehested, J,; Sehested, K.; Nielson, O. J,; Wellington, T.T. *J. Phys. Chem.* 1994, 98, 6731.

16. Howard, C.J. *J. Phys. Chem.* **1979,** 83, 3.

17. Brown, R.L. *J. Res. Natl. Bur. Stand (U.S)* **1978**, 83, 1.

18. Keyser, 1.. F.; Moore, S. B.; Leu, M.T. *J. Phys. Chem.* **1991,95,5496.**

19. Fuller, E.N.; Schettle, P.D.; Giddings, J.C. *Ind. and Eng. Chem.* **1966**, *58,* 19.

20. Kim, P.; MacLean, D.].; Valance, W.G.J. *Phsy. Chem* **1980,84,** 1806.

21, Raulch, D.]..; Duxburg, J.; Gront, S."1'.; Montague, D.C. *J. Phys. Chem. Ref. Data* **1981,** 10, Suppl. 1.

22. Turnipseed, A. A.; Birks, J. W. *J. Phys.* hem. 1991,95,6569.

23. Howard, M. J.; Smith, I.W.M. *Prog. React. Kinet.* 1983,12,55.

24. Mozurkewich, M.; Benson, S.W. *J. Phys. Chem. 1984,88,6429.*

25. DeMore, W.B.; Sander, S.P.; Golden, D.H.; Hampson, R.F.; Kurylo, M. J.; Howard, C. J.; Ravishankara, A. R.; Kolb, C.E.; Molina, M.J. *Chemical Kinetics and Photochemical Data for Use in Stratospheric Modeling*, Evaluation Number 10, JPL Public at ion 92-20; Jet Propulsion Laboratory, California institute of Technology, Pasadena, CA.

26. Troe, J. *J. Chem. Phys. 1977,66,4745.*

27. '1'roe, J. *J. Chem. Phys.* 1977,66,4758.

28. Patrick, R.; Golden, D.M. *Int. J. Chem. Kin. 1983,* 15.1189.

29. Tsang, T.; Hampson, R.F.J. *J. Phys. Chem. Ref. Data. 1986, 15,* 1087.

30. Stedmam, D.H.; Niki, H. *Environ. Lett. 1973,4,303.*

31. Francisco, J. S.; Zhao, Y.; Lester, W.A. Jr.; William, I.H. *J. Chem. Phys.* 1992,96,2861.

32. Bedzhanyan, Y. R., Markin, E. M. and Gershenzon, Y. M., *Kinet. Catal. 1992,* 33, 591.

Table 1. Observed mass spectral intensities of FO_2.

Ion	m/c	electron impact energy (eV)							
		30	40	50	60	70	80	90	100
~@+-/~o+-	51/35	4.5	2.3	2.0	1.9	2.0	2.1	2,1	2.0

a. Emission current was 3.0 mA.

Table 2. Summary of rate coefficients and rate parameters for reactions of FO_2 with NO, N02, O_3, CH4, and C_2H_6, and reaction of FO with O_3.

Reaction	T (K)	k x 10^{13} (cm^3 molecule-1 s-1)	A, (cm^3 $molecule^{-1}$ s-l)	E/R (K)
FO_2 + NO → products	298	8.5±1.3(175)[a]	(7.5±5)x10^{-12}	688±145
	270	5.2*1.8(25)		
	240	4.1±1.6(26)		
	220	3.2±1.5(25)		
	190	2.1±1.3(33)		
	298[b]	14 7±0.8		
FO_2 + N02 → products	315	.52±.10(16)	(3.8±.8)x10^{-11}	2042±56
	298	.42*,08(18)		
	273	.24±.05(14)		
	260	13±. 10(34)		
	298b	1.05±.1 5		
FOB + 03 → products	298	< 3x10^{-2}		
	298b	<3.4x10-3		
FO + 03 → products	298	< 0.1		
	298b	<12		
	298c	< 2x1 0-3		
F02 + CH_4 → products	298	< 2x10^{-3}		
	298b	< 4.1x10^{-2}		
FO_2 + C_2H_6 → products	298	<4x1()-3		

a. Number of experimental measurements are given in parenthesis.
b. Ref. 15.
c. Value inferred from the work of Bedzhanyan et al. (ref 32)

Table 3. Comparison of rate coefficients (cm^3 $molecule^{-1}$ s^{-1}) for some reactions involving X02 at room temperature.

	HO_2	F02b	03
NO	8.6×10^{-12}a	8.5 x10-13	1.8×10^{-14}a
N02	5×10^{-15}a	4.2×10^{-14}	3.2×10^{-17}a
O_3	2×10^{-15}a	$< 3 \times 10^{-15}$	-
CH_4	7.1×10^{-27}c	$< 2 \times 10^{-16}$	$< 1.2 \times 10^{-21}$d
C_2H_6	5.4×10^{-24}c	$< 4_x 10^{-16}$	

a. Ref. 25.
b. This work.
c. Ref. 29.
d. Ref. 30.

Figure Captions:

Figure 1. Schematic of the discharge-flow mass spectrometer apparatus for kinetics study of FO_2 reactions.

Figure 2. F02 decay in the presence of NO at 298 K. Numbers arc NO concentrations (1 013 molecule cm^{-3}).

Figure 3. First-order decay rates, k^1, of F02 as function of [N02] at 298 K (○), 270 K (●), 240 K (□), 220 K (▼), and 190 K (V).

Figure 4. Temperature dependence of k_{11}

Figure 5. FO_2 decay in the presence of N02 at 298 K. Numbers are N02 concentrations (1 014 molecule cm^{-3}).

Figure 6. First-order decay rates, k^1, of F02 as function of [N02] at315 K (▼), 298 K (0), 273 K (●), and 260 K (V).

Figure 7. Temperature dependence of k_{12}.

Figure 8. Highest occupied molecular orbital (}IOMO) of H02 and FO_2 at 2A" ground state,

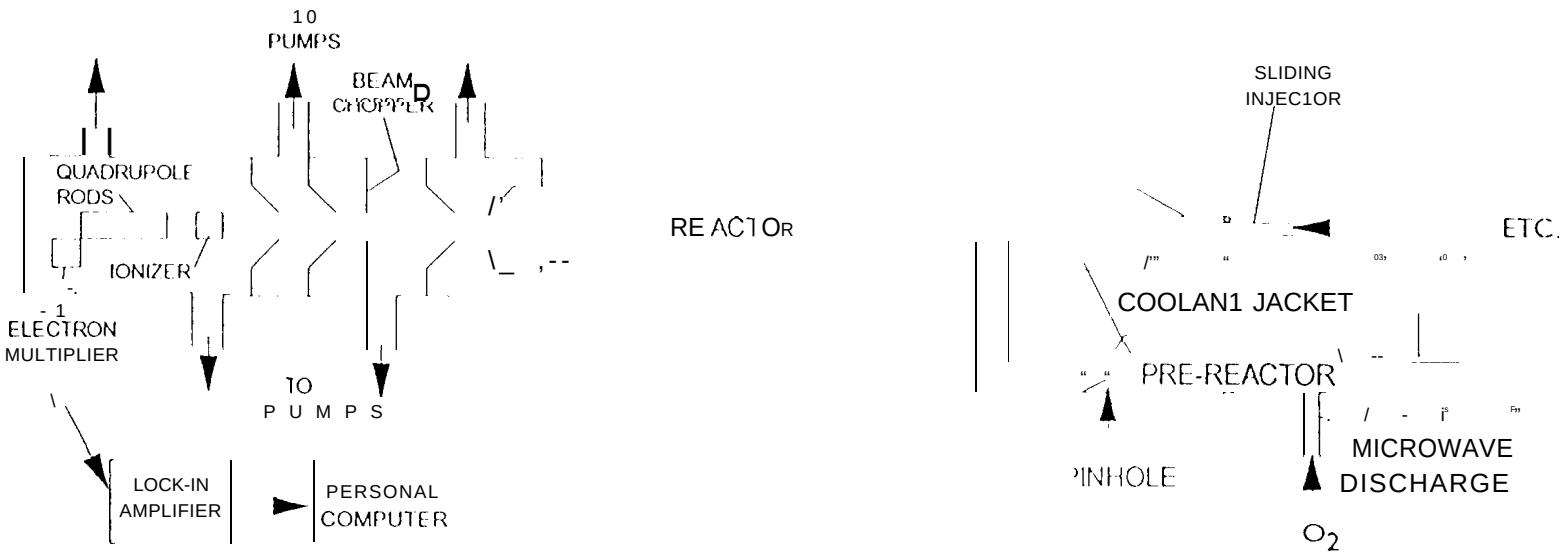
10
PUMPS
BEAM
CHOPPER
QUADRUPOLE
RODS
IONIZER
ELECTRON
MULTIPLIER
TO
P U M P S
LOCK-IN
AMPLIFIER
PERSONAL
COMPUTER
RE ACTOR
SLIDING
INJEC1OR
ETC.
COOLAN1 JACKET
PRE-REACTOR
MICROWAVE
DISCHARGE
O_2

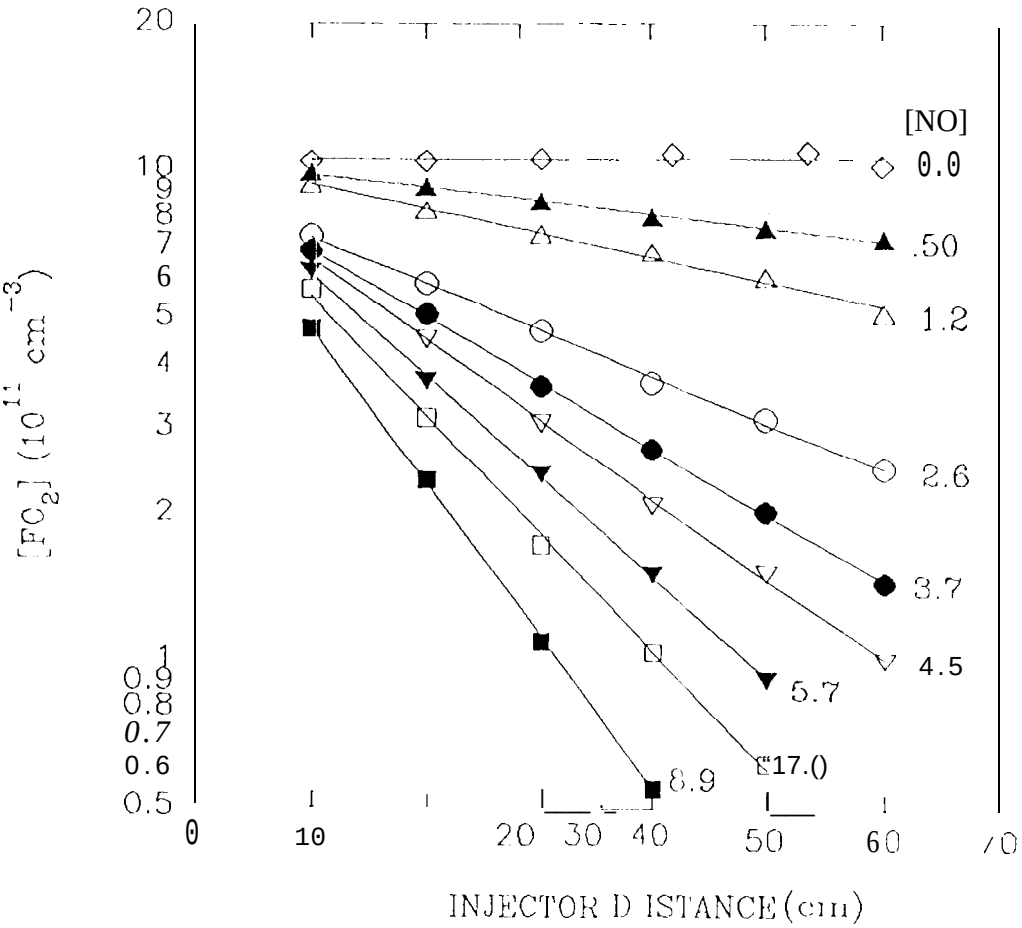
20
10
9
8
7
6
5
4
3
2
1
0.9
0.8
0.7
0.6
0.5
[FO2] (10^11 cm^-3)
[NO]
0.0
.50
1.2
2.6
3.7
4.5
5.7
8.9
0
10
20
30
40
50
60
INJECTOR D ISTANCE (cm)

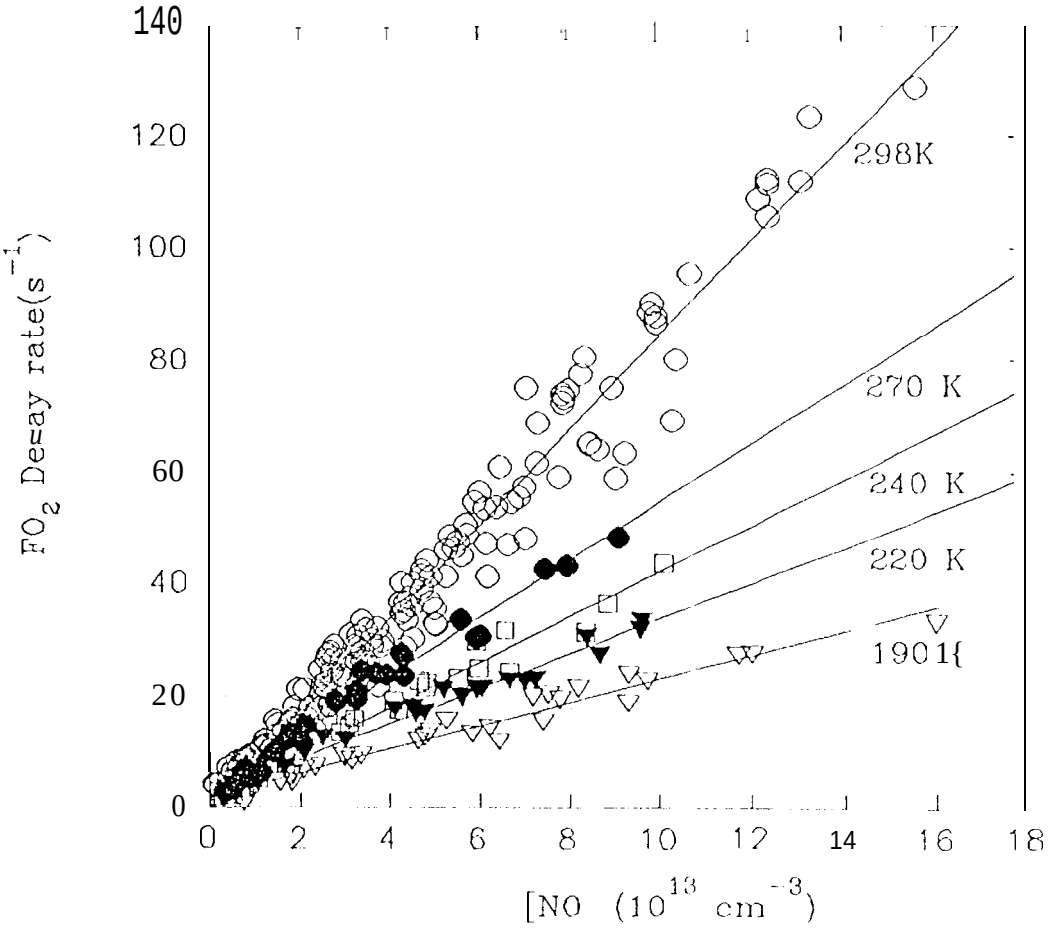
140
120
100
80
60
40
20
0
0
2
4
6
8
10
12
14
16
18
298K
270 K
240 K
220 K
190K
FO_2 Decay rate(s^{-1})
[NO (10^{13} cm^{-3})

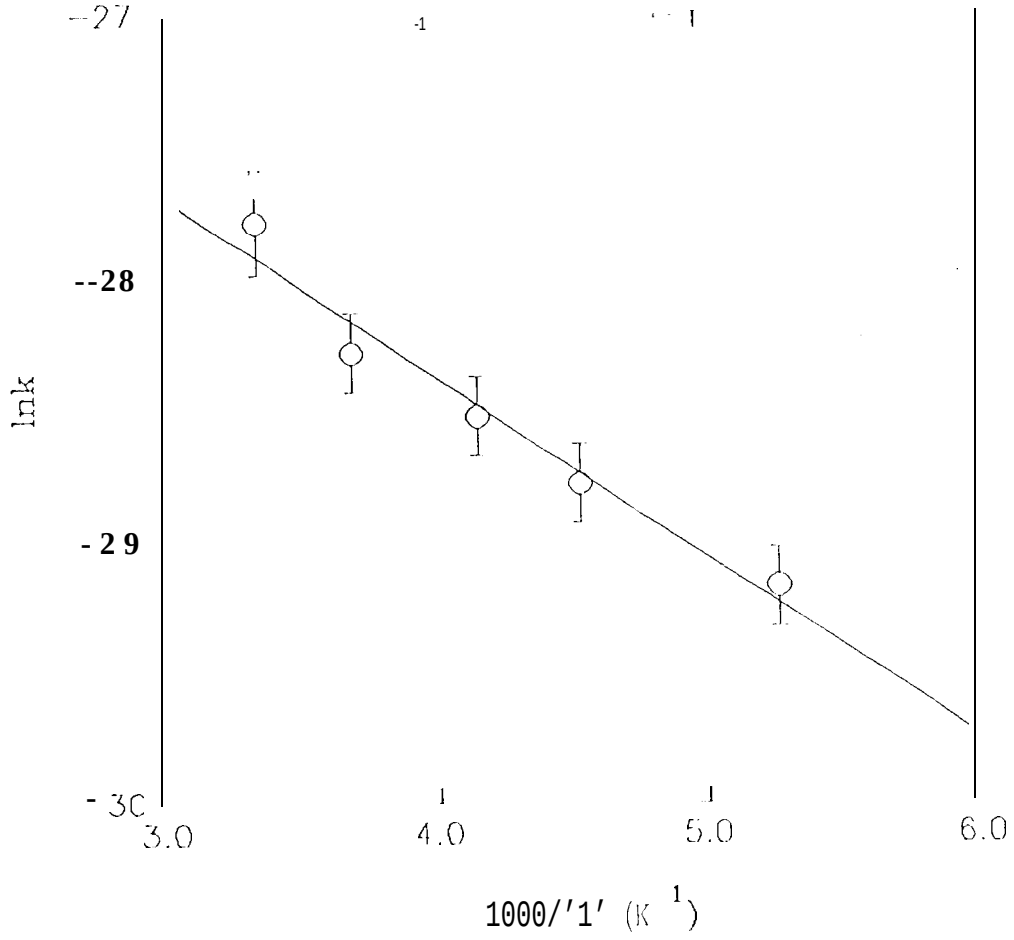
-27
--28
- 2 9
- 3C
lnk
3.0
4.0
5.0
6.0
1000/'1' (K 1)

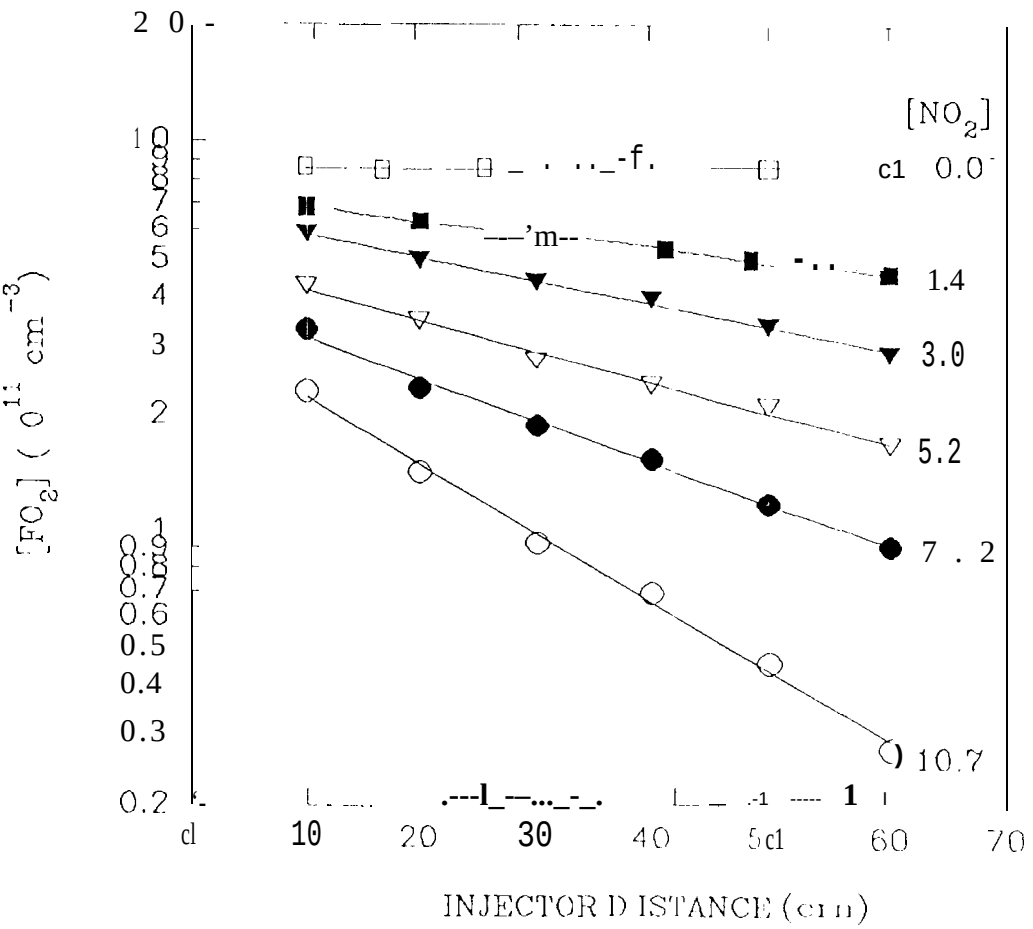
[NO2]
1.4
3.0
5.2
7.2
10.7
[FO2] (10^11 cm^-3)
INJECTOR DISTANCE (cm)

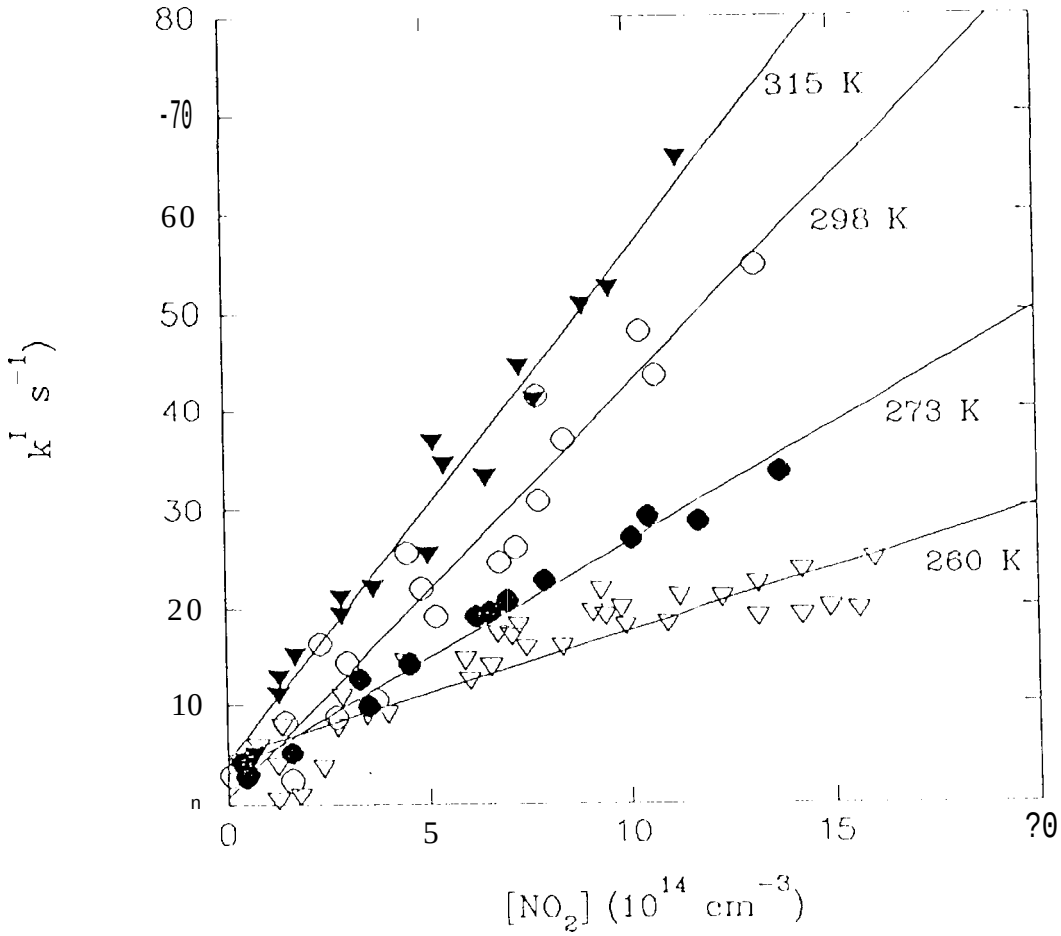
80
-70
60
50
40
30
20
10
n
0
5
10
15
?0
315 K
298 K
273 K
260 K
k^I s^{-1})
[NO_2] (10^{14} cm^{-3})

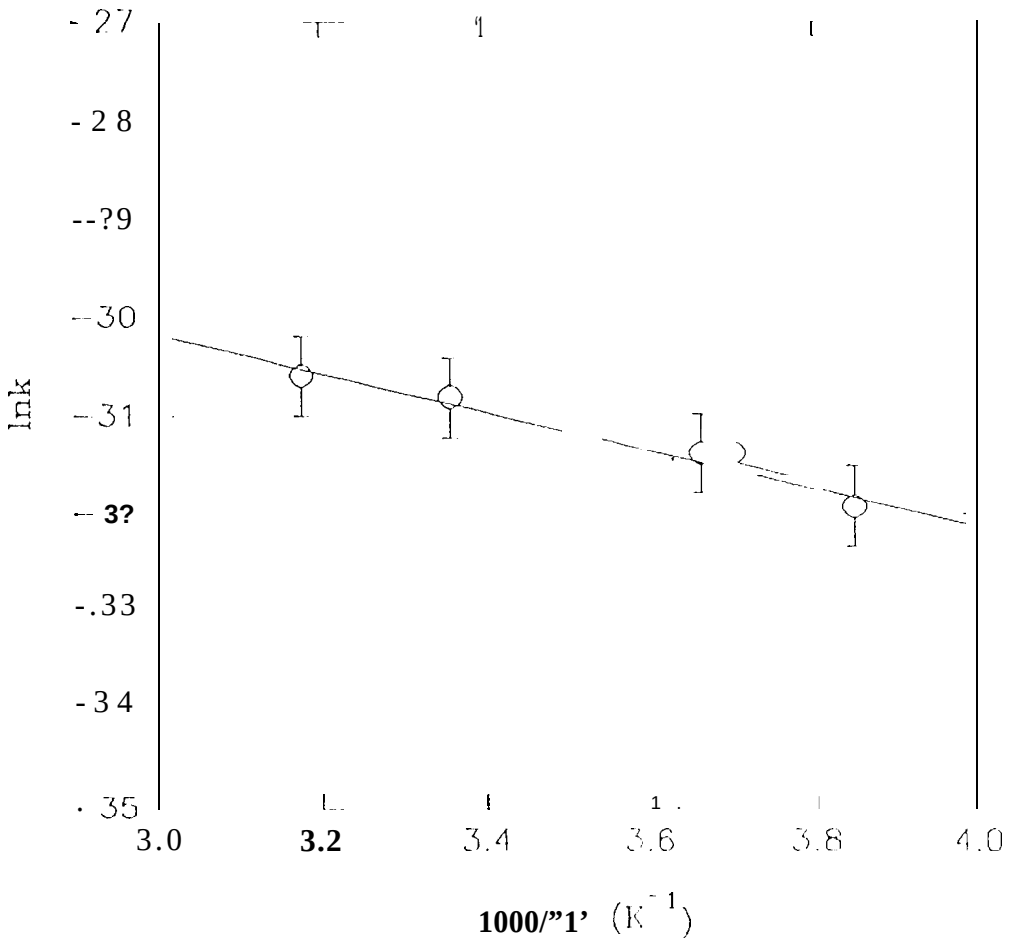
- 27
- 2 8
--?9
--30
lnk
- 31
-- 3?
-.33
- 3 4
. 35
3.0
3.2
3.4
3.6
3.8
4.0
1000/"1' (K⁻¹)

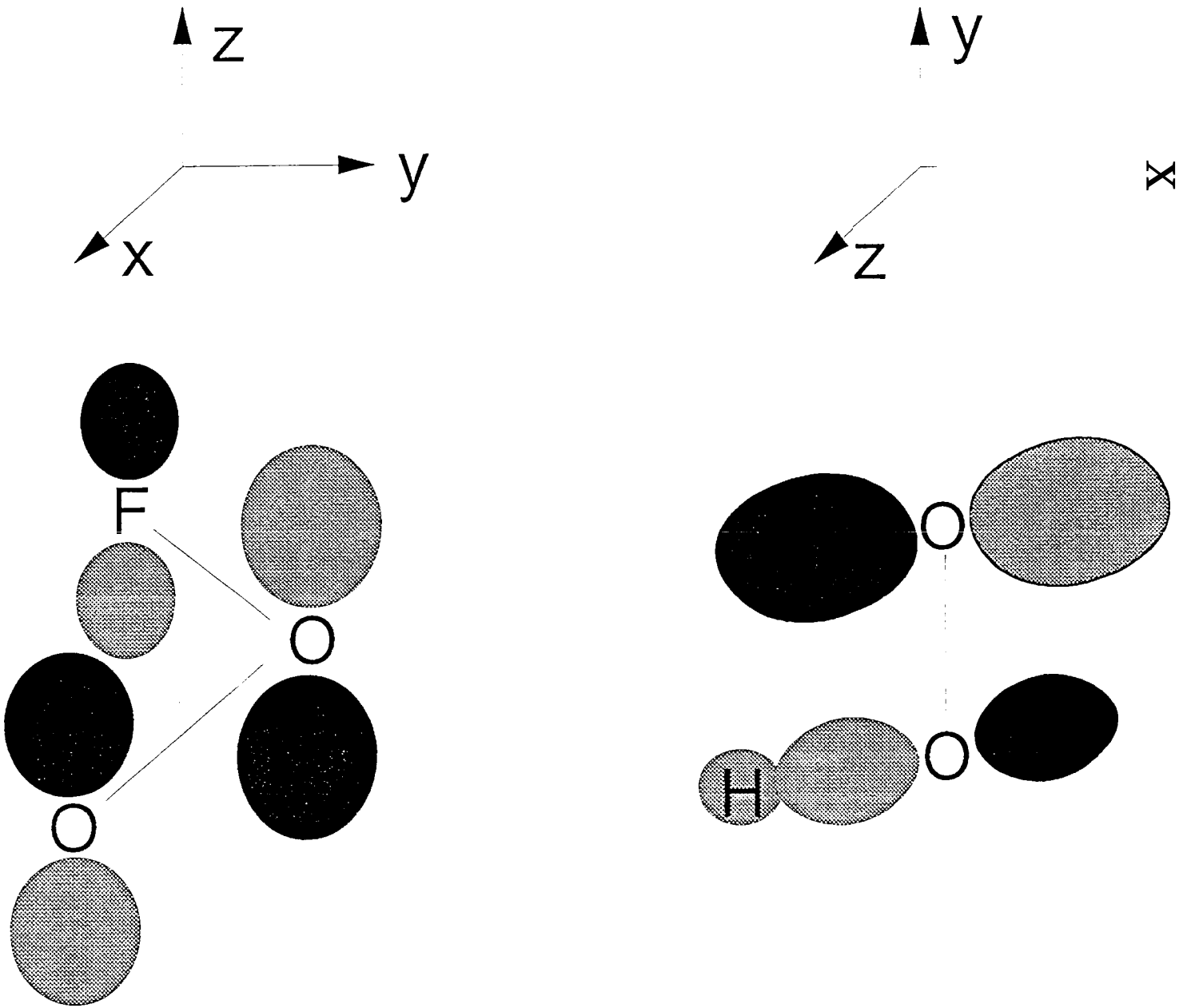
z
y
x
F
O
O
y
x
z
O
H
O